A New Model to Describe Puffing and Microexplosion of Single Titanium(IV) Isopropoxide/*p*-Xylene Droplets in Hot Convective Air

P. Narasu, E. Gutheil*

Interdisciplinary Center for Scientific Computing, Heidelberg University,
69120 Heidelberg, Germany
*Corresponding author: gutheil@iwr.uni-heidelberg.de

Abstract

In flame spray pyrolysis, the precursor solution droplet undergoes heating and evaporation, followed by gas phase combustion and generation of nanoparticles. Depending on the precursor solution considered, the precursor/solvent droplet may experience puffing and microexplosion. The present study concerns single precursor/solvent droplets of titanium(IV) isopropoxide (TTIP) in *p*-xylene at room temperature in hot convective air at atmospheric pressure. A new one-dimensional model is used to describe the processes in the spherically symmetric droplet interior with emphasis on the puffing and the microexplosion. After the initial droplet heating, the preferential evaporation of the higher volatile component causes the accumulation of the lower volatile precursor at the droplet surface, and thus forms a liquid shell that hinders the evaporation process. In the droplet interior, the higher volatile component accumulates and when the temperature reaches the boiling point of that liquid, puffing and microexplosion of the droplet occur once the pressure inside the droplet exceeds the ambient pressure. A parameter study is performed to show the dependence of the puffing and the microexplosion on the initial precursor loading, the initial droplet size, the ambient gas temperature, and the relative velocity between the droplet and the ambience. There are situations where microexplosion follows the puffing or puffing repeats until the end of the droplet lifetime with no microexplosion. This is the first model to successfully describe the puffing in precursor solution droplets.

Keywords

Puffing, Microexplosion, Precursor/solvent droplet, Titanium(IV) isopropoxide, *p*-xylene

Introduction

Flame spray pyrolysis (FSP) is a powerful technique to syntesize a wide variety of nanoparticles, which may be designed to meet the requirements of the potential application. During the generation of nanoparticles using spray flames, occurrence of puffing and microexplosion of the precursor/solvent droplets is found in experiment [1]. Therefore, it is important to understand the puffing and microexplosion phenomena of the precursor solution droplet, since it may have a significant impact in enhancing the vaporization of the liquid in FSP.

There is a number of experimental studies on microexplosion. Stodt et al. [1] used high-speed camera imaging technique and confirmed the occurrence of microexplosions of precursor solution droplets during the synthesis of nanoparticles using spray flames. Li et al. [2] experimentally studied the microexplosion of single isolated burning droplets using titanium(IV) isopropoxide (TTIP) as the precursor and xylene as the solvent. It was found that the reason for the microexplosion of the TTIP/xylene droplet is due to the accumulation of the lower volatile TTIP at the droplet surface. Also, the higher volatile xylene in the droplet interior below the liquid shell is heated, which increases the pressure inside the shell before microexplosion occurs.

Recently, the processes of puffing and microexplosion in composite kerosene, diesel, and rapeseed oil/water droplets was studied experimentally by Fedorenko et al. [3]. They also used a numerical model in which a water sub-droplet is located in the center of the fuel/water droplet and the heating process of the composite droplet is based on the analytical solution of the one-dimensional heat transfer equation, and the mass evaporation rate of the fuel is calculated

using the Abramzon-Sirignano model [4]. The time to the puffing or microexplosion, which were not distinguished, showed good agreement with the experimental results. Li et al. [5] employed optical techniques including interferometric particle imaging and standard rainbow refractometry to understand the droplet microexplosion during single droplet combustion of the tin(II) 2-ethylhexanoate/xylene precursor/solvent system. Also, a multicomponent diffusion-limit model was developed to simulate the experimental changes of droplet size and rainbow pattern. It was concluded that increasing the initial concentration of the precursor speeds up the occurrence of the droplet micro-explosions by accelerating the accumulation of the precursor at the surface of the droplet. Ren et al. [6] studied the microexplosion (without puffing) of a tin(II) 2-ethylhexanoate/*m*-xylene droplet, where one-dimensional equations were solved to describe the mass and heat transfer inside the droplet and the thermophysical properties of the precursor were approximated. They found shorter microexplosion times for droplets with larger initial precursor concentrations.
Puffing has not yet been addressed in numerical simulations even though it seems to be an important predecessor of microexplosion in precursor solvent droplets [1]. In the present study, both puffing and microexplosion of the titanium(IV) isopropoxide (TTIP) in *p*-xylene droplets are addressed, which may be used to produce TiO_2 nanoparticles.

Mathematical Model
A spherically symmetric precursor solution droplet is exposed to an ambience of hot convective air at atmospheric pressure. Low droplet Reynolds numbers up to about twenty are considered, which ensure that there is neither inner recirculation of the droplet nor flow separation in the wake of the droplet so that a one-dimensional model may be used. For the liquid precursor/solvent droplets of TTIP/*p*-xylene, the droplet heating and evaporation are described using the conduction-limit and the diffusion-limit models, respectively. In order to include the puffing and microexplosion into the model, these equations are modified follwoing the study by Grosshans et al. [7], which was motivated by Nešić and Vodnik [8], who studied the solid layer formation of droplets during spray drying processes. The droplet is assumed to remain spherical all the times, the solubility of air in the liquid is neglected, the gas phase is in a quasi-steady state, the droplet evaporates in a non-reacting inert environment, and heat transfer due to radiation is assumed negligible [9]. The real behavior of the TTIP/*p*-xylene droplets is considered through the use of appropriate activity coefficients [10, 11], which are modeled using the non-random two-liquid (NRTL) method.
The one-dimensional equations include the conduction-limit and the diffusion-limit models for the temporal and spatial variations of the temperature and the species concentrations inside the multi-component droplet. The model for the puffing and possible microexplosion of the precusor solution droplets is based on the fact that the component with the lower volatility accumulates at the droplet surface, building up a liquid shell of thickness δ. The mass evaporation is hindered by this shell similar to the crust formation in case of the process of droplet drying [7].
The equation describing the mass evaporation rate $\dot{m}_i$ of component i yields

$$\dot{m}_i = \frac{2\pi r_{\mathrm{d},i} \rho_{\mathrm{f}} D_{\mathrm{f},i} \widetilde{\mathrm{Sh}} \ln(1 + B_{\mathrm{M},i})}{1 + \frac{\widetilde{\mathrm{Sh}} D_{\mathrm{f},i}}{2 D_{\mathrm{sh}}} \frac{\delta}{r_{\mathrm{d}} - \delta}} \tag{1}$$

with the Spalding mass transfer number [9] $B_{\mathrm{M},i} = \dfrac{Y_{\mathrm{s},i} - Y_{\infty,i}}{1 - Y_{\mathrm{s},i}}$, $i = 1, 2$. Here, $r_{\mathrm{d},i}$ denotes the instantaneous droplet radius of component i, ρ_{f} is the density of the mixture in the film, $D_{\mathrm{f},i}$ denotes the diffusivity of the component i into air in the film, $Y_{\mathrm{s},i}$ is the mass fraction of the component i at the surface, and $Y_{\infty,i}$ is the mass fraction of the component i in the ambience. $\widetilde{\mathrm{Sh}}$ is the modified Sherwood number [4] and D_{sh} accounts for the diffusivity of the vapor in the liquid shell. $\delta(t)$ is the thickness of the liquid shell, which varies with time as

$$\delta(t) = [1 - Y_{\mathrm{TTIP,s}}(t)]\, r_{\mathrm{d}}(t), \tag{2}$$

where $Y_{\mathrm{TTIP,s}}$ is the mass fraction of TTIP at the surface of the droplet when the spatial average temperature, $\overline{T}$, of the droplet reaches the boiling point of the higher volatile component *p*-xylene, and $r_{\mathrm{d}}(t)$ denotes the droplet radius at time t. Thus, once the liquid shell is formed, its thickness varies with time, depending on the droplet heating and evaporation processes. $\overline{T}$ is calculated as

$$\overline{T} = \frac{\sum_{j=1}^{N} T_{\mathrm{l},j}}{N}, \tag{3}$$

where j stands for the grid point, N represents the number of grid points and T_{l} is the droplet temperature at the respective grid point. It is to be noted that, before the liquid shell is formed, $\overline{T}$ repesents the spatial average temperature of the entire droplet and, after the formation of the liquid shell, $\overline{T}$ denotes the spatial average temperature of the droplet interior the liquid shell. The energy balance at the droplet surface considering the liquid shell thickness δ is given by

$$4\pi {r_{\mathrm{s}}}^2 \frac{\partial(\lambda_{\mathrm{l}} T)}{\partial r}\bigg|_{r=r_{\mathrm{s}}} = \frac{4\pi {r_{\mathrm{s}}}^2 h(T_{\mathrm{g}} - T_{\mathrm{s}})}{1 + \frac{\widetilde{\mathrm{Nu}}\lambda_{\mathrm{f}}}{2\lambda_{\mathrm{sh}}} \frac{\delta}{r_{\mathrm{d}} - \delta}} - L_{\mathrm{v}}(T_{\mathrm{s}})\dot{m}, \tag{4}$$

where λ_{l} is the thermal conductivity of the liquid mixture, h stands for the heat transfer coefficient, T_{g} is ambient gas temperature, T_{s} is the droplet surface temperature, and L_{v} represents the temperature-dependent latent heat of vaporization of the liquid mixture at the surface temperature T_{s} of the droplet. In analogy to mass transfer, the denominator the first term on the right-hand side of Eq. (4) including the liquid shell thickness can be interpreted as the resistance for heat transfer in the film and the resistance of the liquid shell, where, $\widetilde{\mathrm{Nu}}$ is the modified Nusselt number [4] incorporated to account for the convective effects in heat transfer, λ_{f} denotes the thermal conductivity of the gas mixture in the film, and λ_{sh} accounts for the thermal conductivity in the liquid shell. The thermophysical properties are taken from Narasu et al. [11].

Results and Discussion

The heating, evaporation, puffing, and possible microexplosion of a single droplet consisting of a precursor solution of TTIP and *p*-xylene are investigated for the initial conditions chosen based on the experimental study of Schneider et al. [12].

The initial droplet radius is 50 µm with a relative velocity of 4 m/s between the droplet and the ambience at an ambient temperature of 1200 K for the initial TTIP mass fraction of 0.25. The left part of Fig. 1 displays the temporal profiles of the normalized droplet surface area $(d/d_0)^2$ and liquid shell thickness δ, and the right part displays the temporal evolution of the liquid mass fractions of p-xylene and TTIP and the temperature at the droplet surface and at the center of the droplet, as well as the spatial average temperature, $\overline{T}$ inside the droplet. Initially, the droplet expands due to heating, see left part of Fig. 1, reflecting the variable liquid properties used in the model. At the droplet surface, the droplet heats up which causes the higher volatile

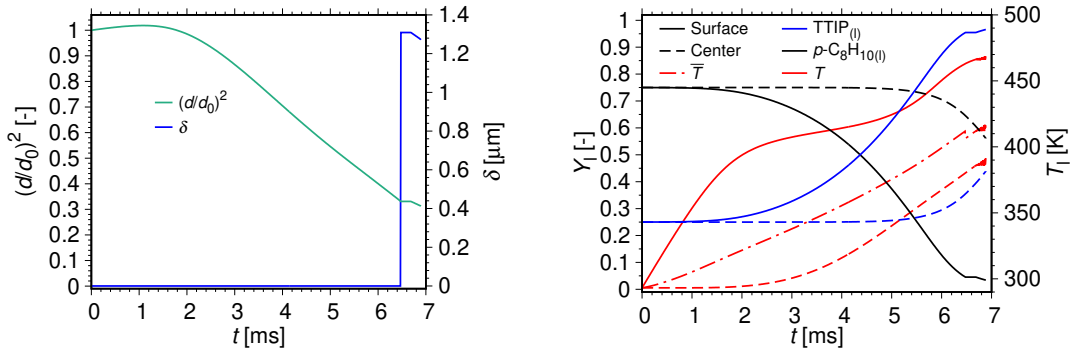

Figure 1. Left: Normalized droplet surface area and variation of the liquid shell thickness with time. Right: Mass fractions of species and droplet temperature at the center and surface of the droplet and spatially averaged droplet temperature, $\overline{T}$. Initial conditions: $r_{\mathrm{d},0}$ = 50 µm, $T_{\mathrm{l},0}$ = 293.15 K, p = 1 bar, u_0 = 4 m/s, $T_{\mathrm{g},0}$ = 1200 K, $Y_{p\text{-}\mathrm{C_8H_{10},0}}$ = 0.75, $Y_{\mathrm{TTIP},0}$ = 0.25.

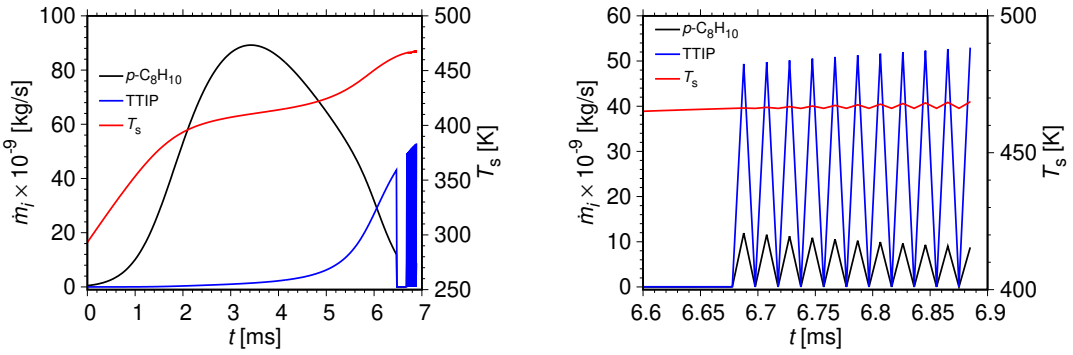

Figure 2. Left: Mass evaporation rates and droplet surface temperature with time. Right: Zoomed view. Initial conditions: $r_{\mathrm{d},0}$ = 50 µm, $T_{\mathrm{l},0}$ = 293.15 K, p = 1 bar, u_0 = 4 m/s, $T_{\mathrm{g},0}$ = 1200 K, $Y_{p\text{-}\mathrm{C_8H_{10}},0}$ = 0.75, $Y_{\mathrm{TTIP},0}$ = 0.25.

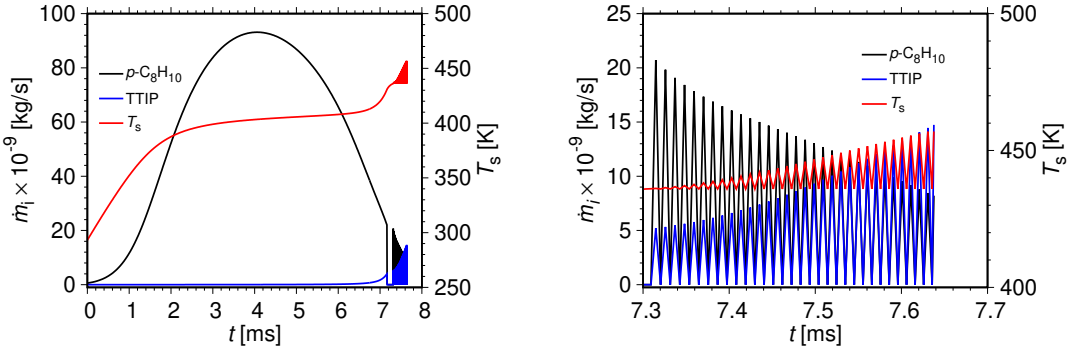

Figure 3. Left: Mass evaporation rates and droplet surface temperature with time. Right: Zoomed view. Initial conditions: $r_{\mathrm{d},0}$ = 50 µm, $T_{\mathrm{l},0}$ = 293.15 K, p = 1 bar, u_0 = 4 m/s, $T_{\mathrm{g},0}$ = 1200 K, $Y_{p\text{-}\mathrm{C_8H_{10}},0}$ = 0.975, $Y_{\mathrm{TTIP},0}$ = 0.025.

p-xylene to evaporate, resulting in the increase in the mass fraction of TTIP. At the center of the droplet, the temperature and the mass fraction of TTIP are lower and that of *p*-xylene is higher compared to their corresponding values at the droplet surface, see right part of Fig. 1, due to the diffusive nature of the processes occurring inside the droplet.

At 6.48 ms, the spatial average temperature, $\overline{T}$, reaches the boiling point of 412 K of *p*-xylene, cf. right part of Fig. 1, after which the liquid shell is formed due to the accumulation of the precursor at the droplet surface, hindering the droplet evaporation process as can be observed from the slight increase in the normalized droplet surface area, see left part of Fig. 1, which goes along with an increase of the thickness of the liquid shell. Such an increase in the droplet size is also reported in previous studies related to microexplosion of TTIP/xylene [2] and water/fuel [3] droplets. $\overline{T}$ drops somewhat due to the formation of the liquid shell, see right part of Fig. 1.

Figure 2 displays the mass evaporation rates of TTIP and p-xylene as well as the droplet surface temperature where the right part is a zoom of the left part. As soon as $\overline{T}$ reaches the boiling point of *p*-xylene once again at 6.69 ms, see left part of Fig. 1, puffing starts releasing the resistance to evaporation. This is reflected in the mass evaporation rate of both components and the droplet temperatures at the center and the surface and in $\overline{T}$ displayed in the zoom part of Fig. 2 and the right part of Fig. 1. After the first puff, these processes repeat, leading to a sequence of ten puffs after which microexplosion occurs at 6.89 ms during which the droplet is completely evaporated due to the pressure rise inside the droplet reaching above the ambient pressure. With the onset of puffing, the shell thickness decreases due to the reduction in the droplet size as shown in the left part of Fig. 1.

Figure 3 shows numerical results of the same conditions as displayed in Fig. 2 with a reduction of the initial TTIP mass fraction from 0.25 to 0.025. This reduction leads to a longer droplet lifetime and a later start of the puffing, which is due to the delay of the spatial average droplet temperature in reaching the boiling point of the p-xylene as is evident from the left parts of Figs. 2 and 3. In the case of reduced initial TTIP mass fraction, puffing starts at 7.31 ms and

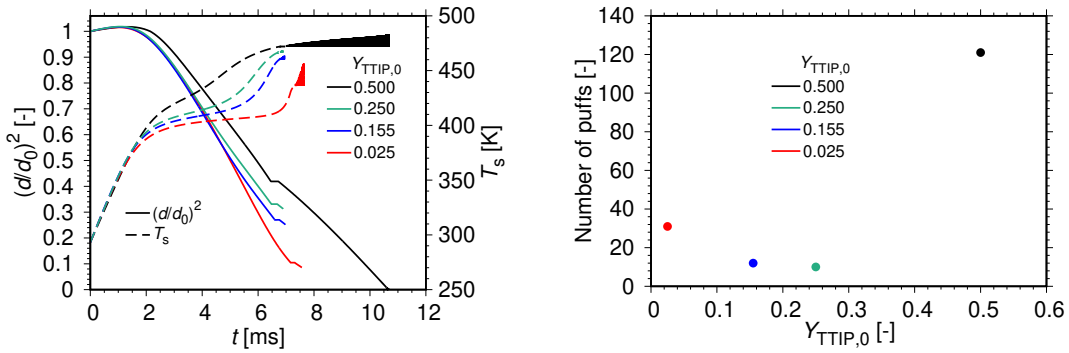

Figure 4. Left: Normalized droplet surface area and droplet surface temperature with time. Right: Number of puffs for different initial precursor mass fractions. Initial conditions: $r_{d,0}$ = 50 µm, $T_{l,0}$ = 293.15 K, p = 1 bar, u_0 = 4 m/s, $T_{g,0}$ = 1200 K.

the microexplosion occurs at 7.63 ms. There are 31 puffs in case of the initial mass fraction of 0.025 compared to ten before microexplosion occurs, doubling the frequency at which they occur, and it is most challenging that the peak values of the mass evaporation rates decrease for p-xylene and increase for TTIP whereas in the case of 0.25, both maxima of the mass evaporation rates attain more or less constant values. The enhancement of vaporization of TTIP is a consequence of the increase in droplet surface temperature for the lower TTIP mass loading as can be seen in the right part of Fig. 3. The number of puffs and the droplet lifetimes are strongly dependent on the initial TTIP mass fraction, and a survey is presented in Fig. 4.
The left part of Fig. 4 shows the temporal profiles of the normalized droplet surface area and droplet surface temperature. Increasing the initial mass fraction of TTIP results in faster accumulation of the lower volatile precursor at the droplet surface and thus speeds up the formation of the liquid shell, eventually resulting in the earlier puffing. The number of puffs decreases with the higher initial mass fraction of TTIP as can be seen in the right part of the figure, which is a consequence of the shorter droplet lifetime and a less steep increase in droplet surface temperature. Moreover, with the increase in the initial mass loading of the precursor in the solution, the time span between puffing and microexplosion reduces, leading to earlier droplet microexplosion as has been found in the studies for different precursor solution systems [5, 6]. However, for the TTIP/*p*-xylene droplet with an initial mass fraction of 0.50, the pressure inside the droplet never increases beyond the ambient pressure, and thus, puffing continues until the droplet completely evaporates without the occurrence of microexplosion.

Conclusions

A new one-dimensional model to describe the heating, evaporation, puffing, and possible microexplosion of single spherically symmetric TTIP/*p*-xylene precursor/solvent droplets in hot convective air has been developed. This is the first model to describe puffing in precursor solution droplets. Conditions are identified in which puffing is followed by microexplosion or puffing leads to complete droplet evaporation.
Initially, the precursor solution droplet heats up during which expansion occurs. As the droplet surface temperature increases, preferential evaporation of the higher volatile *p*-xylene leads to an increase in the mass fraction of TTIP, resulting in the formation of a liquid shell at the droplet surface, which hinders evaporation. As the boiling temperature of the higher volatile component is reached in the droplet interior close to the liquid shell, puffing starts with possible repetitions of puffs releasing mass from the droplet through evaporation of both the components. The number of puffs and its frequency increase with a reduction of the initial mass fraction of the TTIP. An increase in initial TTIP mass fraction reduces the time span between puffing and microexplosion, leading to earlier droplet microexplosion. If the pressure in the droplet interior exceeds the ambient pressure, microexplosion of the droplet occurs, which is found for initial mass fractions of TTIP up to 0.25 under the present conditions but not for 0.50 for which puffing continues until the droplet is completely evaporated.

The present model is suitable to describe puffing followed by possible microexplosion of precursor/solvent single droplets in hot convective air, where under certain conditions, no microexplosion occurs and repeated puffs accompany the droplet evaporation until the end of its lifetime. The phenomena of puffing and microexplosion are extremely important in flame spray pyrolysis since they enhance the evaporation of the liquid precursor solution and they may influence the physical and thermochemical properties of the nanoparticle formation, which is an interesting question that should be addressed in future.

Acknowledgements
Funding by the Deutsche Forschungsgemeinschaft (DFG, German Research Foundation) through SPP 1980 - Projektnummer 374463455 is gratefully acknowledged.

References

[1] M.F.B. Stodt, J. Kiefer, and U. Fritsching. Drop dynamics in heterogeneous spray flames for nanoparticle synthesis. *Atomization and Sprays*, 30(11), 2020.

[2] H. Li, C.D. Rosebrock, N. Riefler, T. Wriedt, and L. Mädler. Experimental investigation on microexplosion of single isolated burning droplets containing titanium tetraisopropoxide for nanoparticle production. *Proceedings of the Combustion Institute*, 36(1):1011–1018, 2017.

[3] R.M. Fedorenko, D.V. Antonov, P.A. Strizhak, and S.S. Sazhin. Time evolution of composite fuel/water droplet radii before the start of puffing/micro-explosion. *International Journal of Heat and Mass Transfer*, 191:122838, 2022.

[4] B. Abramzon and W.A. Sirignano. Droplet vaporization model for spray combustion calculations. *Int. J. Heat Mass Transfer*, 32(9):1605–1618, 1989.

[5] H. Li, C.D. Rosebrock, Y. Wu, T. Wriedt, and L. Mädler. Single droplet combustion of precursor/solvent solutions for nanoparticle production: Optical diagnostics on single isolated burning droplets with micro-explosions. *Proceedings of the Combustion Institute*, 37(1): 1203–1211, 2019.

[6] Y. Ren, J. Cai, and H. Pitsch. Theoretical single-droplet model for particle formation in flame spray pyrolysis. *Energy & Fuels*, 35(2):1750–1759, 2021.

[7] H. Grosshans, M. Griesing, T. Hellwig, W. Pauer, H.U. Moritz, and E. Gutheil. A new model for the drying of mannitol-water droplets in hot air above the boiling temperature. *Powder Technology*, 297:259–265, 2016.

[8] S. Nešić and J. Vodnik. Kinetics of droplet evaporation. *Chemical Engineering Science*, 46(2):527–537, 1991.

[9] G. Brenn, L.J. Deviprasath, F. Durst, and C. Fink. Evaporation of acoustically levitated multi-component liquid droplets. *International Journal of Heat and Mass Transfer*, 50(25-26):5073–5086, 2007.

[10] A. Keller, I. Wlokas, M. Kohns, and H. Hasse. Thermophysical properties of mixtures of Titanium (IV) Isopropoxide (TTIP) and p-xylene. *Journal of Chemical & Engineering Data*, 65(2):869–876, 2020. .

[11] P. Narasu, M. Nanjaiah, I. Wlokas, and E. Gutheil. Numerical simulation and parameterization of the heating and evaporation of a titanium(iv) isopropoxide/p-xylene precursor/solvent droplet in hot convective air. *Int. J. Multiphase Flow*, 150:104006, 2022.

[12] F. Schneider, S. Suleiman, J. Menser, E. Borukhovich, I. Wlokas, A. Kempf, H. Wiggers, and C. Schulz. Spraysyn–a standardized burner configuration for nanoparticle synthesis in spray flames. *Review of Scientific Instruments*, 90(8):085108, 2019.